Science Translational Medicine
AAAS

Notch4 Normalization Reduces Blood Vessel Size in Arteriovenous Malformations

Patrick A. Murphy, *et al.*

Sci Transl Med **4**, 117ra8 (2012);
DOI: 10.1126/scitranslmed.3002670

Editor's Summary

Reducing Inflation

Arteriovenous malformations (AVMs) are a class of vascular abnormalities in which arteries connect directly with veins, thus bypassing the capillary beds and diverting blood flow away from tissues. In these vascular diseases, blood vessels, particularly the veins, become inflated in size and eventually rupture, resulting in hemorrhage and ischemia. AVMs, which can be found in any tissue, are particularly problematic in the brain, where surgical options are limited, and they often result in stroke or death. In a tour-de-force study, Murphy *et al*. now show that dialing down Notch4 receptor signaling in established AVMs in mouse brain reduces the size of enlarged blood vessels, resulting in restoration of blood flow to capillary beds and the reversal of hypoxia in mouse brain tissue.

The Notch receptor is a master regulator of arteriovenous development and is up-regulated in AVMs in human brain. Overexpression of a constitutively active form of Notch4 in endothelial cells lining blood vessel walls is sufficient to induce AVMs in mice. In their new work, Murphy *et al*. first wanted to establish whether correction of Notch4 signaling could induce the regression of AVMs. Using their mouse brain AVM model, they obtained four-dimensional imaging data of the mouse brain vasculature viewed through a window cut into the cranium with two-photon fluorescence microscopy. When Notch4 signaling was normalized, they found regression of enlarged AVMs, which became similar in size to capillaries. This shrinkage in size enabled blood flow to return to oxygen-deprived tissues in the mouse brain. Surprisingly, the authors discovered that AVM regression was not induced by loss of endothelial cells, thrombotic occlusion, or vessel rupture. Rather, it required reprogramming of arterial endothelial cells in the enlarged AVM vessels to a venous endothelial cell specification. This reprogramming was activated by a decrease in Notch4 receptor signaling, which prompted arterial endothelial cells to start expressing the venous marker EphB4. These findings suggest that strategies to manipulate Notch receptor signaling in blood vessel endothelial cells may help to shrink AVMs and may be a new approach to treating AVMs and other vascular diseases.

Science Translational Medicine (print ISSN 1946-6234; online ISSN 1946-6242) is published weekly, except the last week in December, by the American Association for the Advancement of Science, 1200 New York Avenue NW, Washington, DC 20005.

VASCULAR DISEASE

Notch4 Normalization Reduces Blood Vessel Size in Arteriovenous Malformations

Patrick A. Murphy,[1]*† Tyson N. Kim,[1]* Gloria Lu,[1] Andrew W. Bollen,[2] Chris B. Schaffer,[3] Rong A. Wang[1]‡

Abnormally enlarged blood vessels underlie many life-threatening disorders including arteriovenous (AV) malformations (AVMs). The core defect in AVMs is high-flow AV shunts, which connect arteries directly to veins, "stealing" blood from capillaries. Here, we studied mouse brain AV shunts caused by up-regulation of Notch signaling in endothelial cells (ECs) through transgenic expression of constitutively active *Notch4* (*Notch4). Using four-dimensional two-photon imaging through a cranial window, we found that normalizing Notch signaling by repressing *Notch4** expression converted large-caliber, high-flow AV shunts to capillary-like vessels. The structural regression of the high-flow AV shunts returned blood to capillaries, thus reversing tissue hypoxia. This regression was initiated by vessel narrowing without the loss of ECs and required restoration of EphB4 receptor expression by venous ECs. Normalization of Notch signaling resulting in regression of high-flow AV shunts, and a return to normal blood flow suggests that targeting the Notch pathway may be useful therapeutically for treating diseases such as AVMs.**

INTRODUCTION

Abnormally enlarged high-flow blood vessels often continue to expand, leading to life-threatening ruptures. These dangerous vascular lesions underlie the pathology of a wide range of "high-flow" vascular diseases such as arteriovenous (AV) malformations (AVMs), hereditary hemorrhagic telangiectasia, and aneurysms (*1*). The hemodynamic stress exerted on the vasculature by these high-flow lesions can cause hemorrhagic rupture (*1*, *2*). The ability to safely and noninvasively constrict the high-flow large vessels by molecular intervention holds promise to treat these life-threatening conditions for which there are currently limited effective treatments.

Normally, arteries carry blood from the heart to the capillaries through a series of vessels with a successive reduction in caliber to reduce blood flow. Capillaries, where exchange of nutrients and wastes occurs, are the smallest diameter vessels with the lowest blood flow. Postcapillary venules join sequentially wider veins to return blood back to the heart. This AV interface is critical for proper tissue perfusion. High-flow AV shunts are direct connections of arteries to veins, displacing the perfusing capillaries, thus creating positive feedback between increased vessel diameter and accelerated blood flow, and often resulting in vessel rupture. High-flow AV shunts are the fundamental defect in AVMs, causing both tissue ischemia and hemorrhage.

Notch receptors are transmembrane proteins that promote arterial at the expense of venous endothelial cell (EC) specification by enhancing expression of arterial molecular markers, such as *ephrin-B2*, and suppressing the expression of venous markers, such as *EphB4* (*3*). The transmembrane signaling molecule *ephrin-B2* was the first gene found to be expressed by the ECs of arteries but not veins, and is a key marker of arterial ECs (*4*). Its cognate tyrosine kinase receptor, *EphB4*, was the first venous endothelial marker identified (*4*). COUP-TFII, a member of the orphan nuclear receptor superfamily expressed by venous but not arterial ECs, acts upstream of Notch and actively promotes venous EC specification by repressing the expression of Notch (*5*). These AV-distinctive genes are crucial in the morphogenesis of the embryonic vasculature, and their differential expression patterns in arterial and venous vessels persist in adult vascular endothelium (*6*, *7*), suggesting that postnatal retention of AV specification may have a role in maintaining vascular structure and function. Supporting this notion, we and others have reported that Notch activity in the endothelium is aberrantly increased in patients with brain AVMs (*8*, *9*). This suggests that aberrant Notch signaling may be a molecular defect underlying AVMs and that targeting Notch signaling may be a new therapeutic strategy for the treatment of high-flow vascular diseases such as AVMs.

Here, we use a mouse model of Notch-mediated AVMs (*10*) and two-photon excited fluorescence imaging (*11*) to obtain four-dimensional (4D) vascular topology and blood velocity data from the mouse brain vasculature. We demonstrate that high-flow AV shunts can be shrunk to capillary-like vessels after normalization of Notch signaling through an EphB4-dependent mechanism that does not require the loss of ECs.

RESULTS

Repression of *Notch4** causes the specific regression of high-flow AV shunts

In our *Notch4*-Tet* (*Tie2-tTA;TRE-Notch4**) mouse model of AVM, Notch4*, a truncated Notch4 lacking the extracellular domain and thus constitutively active, is expressed specifically in ECs using a temporally regulatable tetracycline-repressible system (*12*). *Notch4** is under the control of the tetracycline-responsive element (*TRE*) and is only activated by the tetracycline transactivator (tTA) driven by the *Tie2* promoter expressed in ECs. Treatment with doxycycline, a tetracycline derivative, led to rapid repression of Notch4* expression to baseline

[1]Laboratory for Accelerated Vascular Research, Division of Vascular Surgery, Department of Surgery, University of California, San Francisco, San Francisco, CA 94143, USA . [2]Department of Pathology, University of California, San Francisco, San Francisco, CA 94143, USA. [3]Department of Biomedical Engineering, Cornell University, Ithaca, NY 14853, USA.
*These authors contributed equally to this work.
†Present address: Koch Institute for Integrative Cancer Research, Massachusetts Institute of Technology, Cambridge, MA 02139, USA.
‡To whom correspondence should be addressed. E-mail: rong.wang@ucsfmedctr.org

levels by 24 hours (fig. S1). Because *Notch4** was rapidly repressed by doxycycline, henceforth, we refer to doxycycline-mediated Notch4* repression simply as *Notch4** repression. *Notch4** expression leads to high-flow AV shunts in the brains of these mice (*10*). To directly test whether these high-flow AV shunts can be normalized after the repression of *Notch4**, we combined two-photon microscopy with a cranial window placed over the right parietal cortex of the mouse brain (fig. S2) to visualize vascular topology and hemodynamics over time.

To avoid the potential confounding effects of hemorrhage and illness in severely affected *Tie2-tTA;TRE-Notch4** mice, we focused on high-flow AV shunts in the mice about postnatal day 12 (P12), when most of the animals had just developed abnormal AV shunts. The minimum diameter of these AV shunts at P11 to P13 averaged 22.2 μm ± SD 7.3, ranging from 8.1 to 51.3 μm (n = 46 shunts in 13 mice), about 2 to 10 times the diameter of the capillaries in age-matched controls, which averaged 4 μm ± SD 0.5, ranging from 2.7 to 5.0 μm (n = 9 capillaries in 3 mice, $P < 0.000002$; Fig. 1, A to D). Centerline flow velocity through AV shunts was much higher than in control capillaries, averaging 37.7 mm/s ± SD 14.4 (n = 11 shunts in 11 mice), compared to 2.1 mm/s ± SD 1.0 in control capillaries (n = 9 capillaries in 3 mice, $P < 0.0000008$; Fig. 1, A to D), and as reported (*13*).

We then analyzed the vessel diameter and blood flow in AV shunts before and after *Notch4** repression. We found that both the diameter and the flow were significantly decreased within 48 hours of Notch4* repression (Fig. 1, E to M) relative to that in untreated mutant animals (fig. S3). The diameter changed primarily in the AV shunt and distal vein; adjacent arterial vessels were less affected (Fig. 1, E to L). To determine whether advanced AVMs also regressed upon Notch4* repression, we examined severely affected, ataxic mice at a later time point (P22) and found that the mature AVMs also regressed (fig. S4).

Not all AV shunts enlarge with continued *Notch4** expression, a variability likely caused by systemic or regional hemodynamic changes. Therefore, we sought to identify a subset of "growth-prone" AV shunts to further test the effects of Notch4* repression. We found that among a growth-prone population of AV shunts, defined by continued growth over several days, all were induced to regress by *Notch4** repression (ten AV shunts in eight mice, fig. S5). In contrast, with continued *Notch4** expression, all of this population continued to grow (five AV shunts in two mice, fig. S5). Supporting these data, we also show similar findings in a separate experiment using mice with a mixed genetic background (fig. S8B).

When imaging for >1 week was possible, we observed the complete regression of the AV shunt such that the AV shunts returned to microvessels resembling capillaries (fig. S6), a finding also confirmed by ex vivo analysis (fig. S6). Structurally, this regression involved the normalization of smooth muscle cell coverage; that is, the wrapping of smooth muscle cells around vessels, typical of arteries, was restored after Notch4* repression (fig. S7). Time point analysis of vessel narrowing indicated that the onset of diameter and velocity reductions occurred within 12 to 24 hours of *Notch4** repression (fig. S8). These data suggest that Notch4* repression results in the prompt narrowing of high-flow AV shunts.

*Notch4** repression directly induces narrowing of AV shunts

Given that reductions in blood flow are known to cause vessel regression (*14*), we asked whether *Notch4** repression leads to shunt regression directly or indirectly through the reduction of AV shunt flow. To discriminate between these possibilities, we measured blood flow in the upstream feeding artery, the AV shunt, and an adjacent artery.

If *Notch4** repression directly reduces the diameter of the AV shunt, we would expect increased resistance and decreased flow through the AV shunt (Fig. 2A). Consequently, the total flow through the feeding artery would also be reduced. Furthermore, the AV shunt blood flow would redistribute to adjacent arteries, thus increasing blood flow in adjacent arteries. Our empirical measurements matched these predictions; total blood flow was reduced, but flow through an adjacent artery to the AV shunt was increased (Fig. 2, B to D).

It is possible that regression of the AV shunt might also be caused indirectly by the effects of reduced flow in the AV shunt after *Notch4** repression (Fig. 2A). Two possible scenarios might lead to reduced flow in the AV shunt. In one, resistance in the adjacent artery is reduced, "stealing" blood flow from the AV shunt. However, in this scenario, total systemic resistance to flow should also be reduced, and thus, combined flow through the AV shunt and the adjacent artery should be increased, which we did not observe. In a second scenario, systemic flow is reduced by events either upstream or downstream of the AV shunt and adjacent artery. However, in this scenario, flow through both the AV shunt and the adjacent artery should be reduced, which we also did not observe. These data suggest that there is a direct mechanism for AV shunt regression after *Notch4** repression.

The mechanism for vessel regression does not require the loss of ECs

To understand the cellular mechanism of AV shunt regression, we asked whether reduction in the total number of ECs or the area covered by individual ECs could be involved. To this end, we used the *ephrin-B2–H2B–eGFP* mouse line to provide nuclear labeling of ECs within the AV shunt (*10*). In the presence of *Notch4**, ECs in the AV shunt, regardless of arterial or venous origin, expressed *ephrin-B2–H2B–eGFP*. The H2B-eGFP (enhanced green fluorescent protein) fusion protein is extremely stable and can persist for months (*15*). Thus, within the AV shunt, in the short time frame of examination, *ephrin-B2–H2B–eGFP* serves as a general EC marker without arterial specificity.

We performed 4D imaging of AV shunt diameters and cell numbers in 23 AV shunts in seven *Tie2-tTA;TRE-Notch4*;ephrin-B2–H2B–eGFP* mice, at time points up to 48 hours after Notch4* repression. Figure 3A shows such an example: AV shunt regression was detected between 20 and 28 hours, but the cell count was not reduced in the regressing AV shunts at 28 hours or even at 36 hours after further vessel regression. Another example is provided in fig. S9. More analysis at 0 and 24 or 28 hours after Notch4* repression showed that all shunts regressed by 40% ± SD 14% by 24 or 28 hours. The onset of AV shunt regression was variable, sometimes occurring as early as 12 hours after Notch4* repression. About 70% (18 of 23) of these AV shunts regressed without detectable loss of cells at 24 or 28 hours, judged by counting the $eGFP^+$ nuclei. These results suggest that AV shunt regression did not depend on the loss of vascular cells. We confirmed that this was the case with an alternative method of tracking EC nuclei using our *Tie2-tTA* induction system in conjunction with a *TRE-H2B-eGFP* reporter. We first verified that this reporter was a specific and robust marker of EC nuclei; analysis of cell labeling in the sections revealed that 91.4% ± SEM 3.4% of 4′,6-diamidino-2-phenylindole–positive ($DAPI^+$) ECs but none of the adjacent mural cells were GFP^+ (fig. S10). We then analyzed vessel diameter and EC number up to 36 hours after Notch4* repression. By 12 hours, we detected vessel regression in 36 of 38 AV shunts

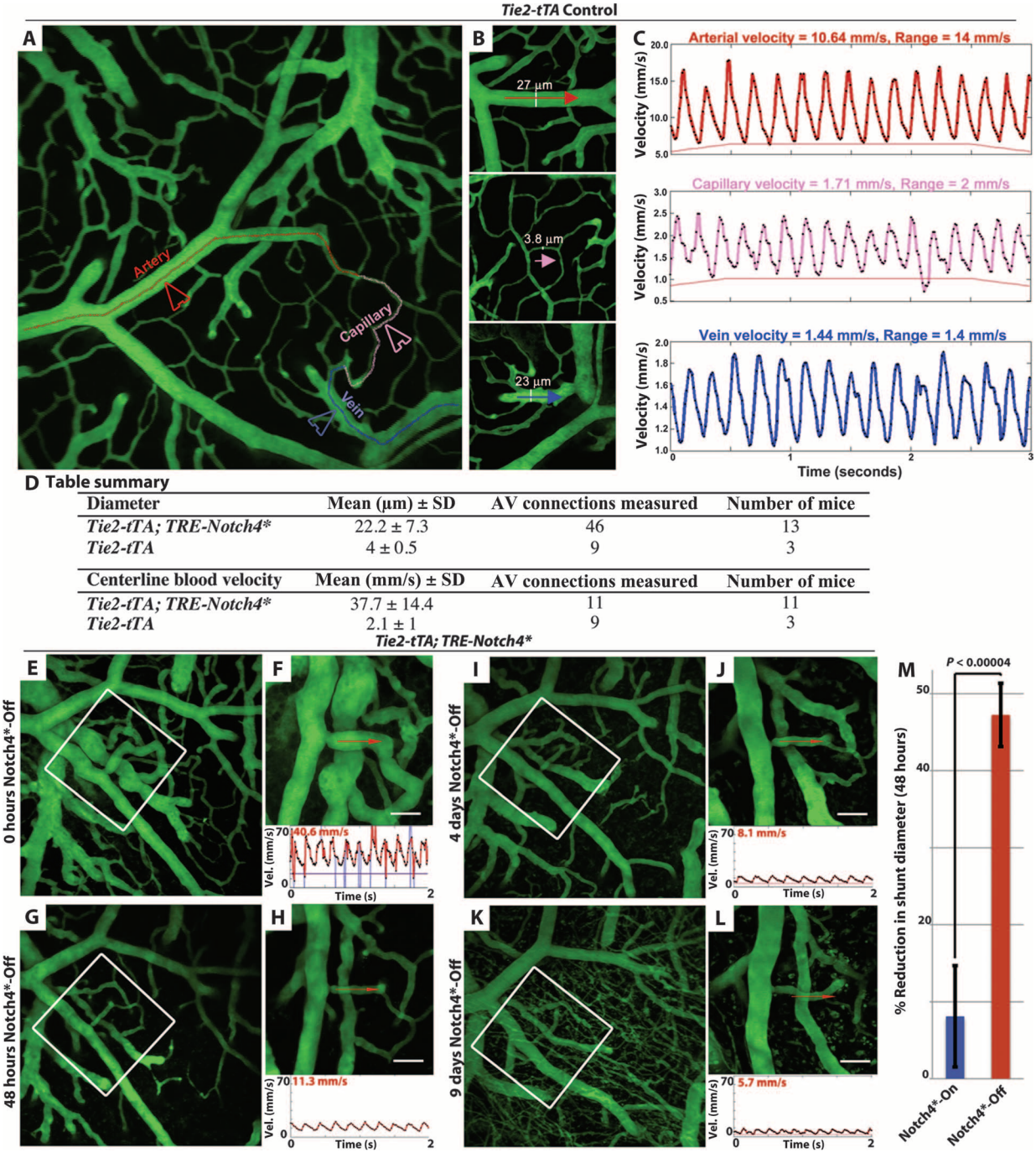

Diameter	Mean (μm) ± SD	AV connections measured	Number of mice
*Tie2-tTA; TRE-Notch4**	22.2 ± 7.3	46	13
Tie2-tTA	4 ± 0.5	9	3

Centerline blood velocity	Mean (mm/s) ± SD	AV connections measured	Number of mice
*Tie2-tTA; TRE-Notch4**	37.7 ± 14.4	11	11
Tie2-tTA	2.1 ± 1	9	3

Fig. 1. Repression of *Notch4** induces the normalization of AVMs. (**A** to **C**) Two-photon time-lapse imaging of cortical brain vessels through a cranial window in wild-type mice. Plasma was labeled by intravenous injection of FITC-dextran. (A) Line depicts the path of blood from artery through arteriole, capillary, venule, and vein. (B) Images of the artery, capillary, and vein in which blood velocity was measured by line scan along the axis are depicted. Diameters of the vessels were measured transaxially. (C) Velocity tracing, as calculated from line scans. Note that both the velocity and the pulse (the range in velocity) were reduced from artery to capillary to vein. (**D**) Table summarizes measurements in control and Notch4* mutant mice. (**E** to **L**) Two-photon time-lapse imaging of cortical brain vessels through a cranial window in *Notch4** mutant mice. Vessel topology was visualized by intravenous FITC-dextran. AV shunts (E and F) were reduced in diameter after the repression of *Notch4** by doxycycline (G to L). Centerline velocity in the regressing AV shunt was obtained by direct measurement of the velocity of individual red blood cells (F, H, J, and L). Repression of *Notch4** decreased blood flow velocity in the AV shunt within 48 hours (compare F to H). (**M**) Quantification of the changes in shunt diameter without repression of *Notch4** (*Notch4**-On) or with repression of *Notch4** (*Notch4**-Off) at 48 hours. Diameter was measured at the narrowest point between artery and vein in *Notch4**-On mice before and after treatment ($n = 22$ AV shunts in 10 mice with and $n = 35$ AV shunts in 11 mice without *Notch4** repression). Reduction in shunt diameter in *Notch4**-On condition is 6% and in *Notch4**-Off condition is 49%. $P < 0.0003$ by Student's t test. Error bars represent SEM between individual AV shunts. Scale bars, 50 μm.

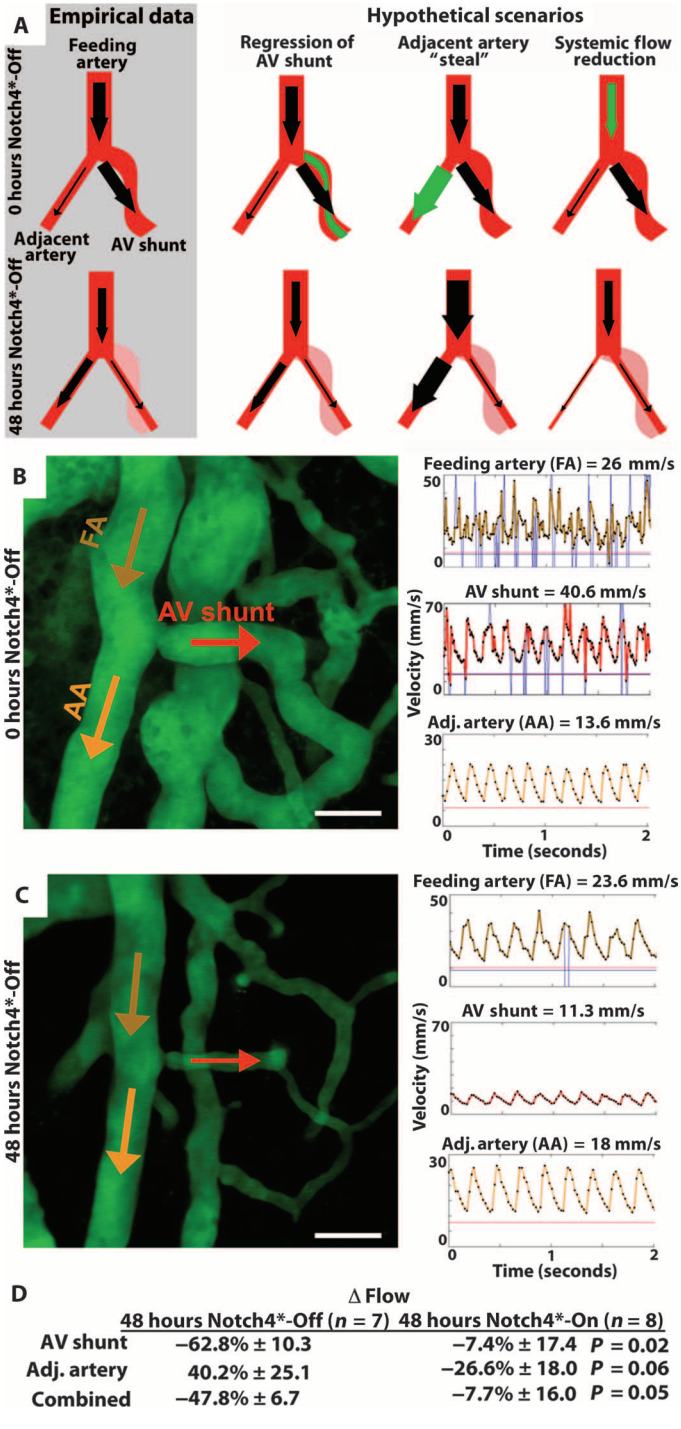

Fig. 2. AVM narrowing is the primary event in AVM regression. (**A**) Illustration of potential ways in which AV shunt regression takes place. The primary event can be either the acute narrowing of the AV shunt or a reduction in flow, caused by either "steal" from an adjacent artery or a systemic reduction in flow. The acute AV shunt narrowing model, predicting the increase in adjacent artery flow and reduction in feeding artery flow, best fits the empirical observations. We do not observe increased feeding artery flow, as predicted by the adjacent artery steal model, or a decrease in adjacent artery flow, as predicted by a systemic flow reduction model. (**B** and **C**) Two-photon time-lapse imaging of cortical brain vessels through a cranial window in *Notch4** mutant mice. Vessel topology was visualized by plasma labeling by intravenous FITC-dextran. Centerline velocity in the regressing AV shunt, feeding artery (FA), and adjacent artery (AA) was obtained by direct measurement of the velocity of individual red blood cells. Repression of *Notch4** decreased blood flow velocity by 48 hours in shunt and feeding artery but increased velocity in the adjacent artery. (**D**) Summary of percent Δ in calculated flow in vessels either 48 hours after *Notch4** suppression or after 48 hours with no *Notch4** suppression. Scale bars, 50 μm.

from the four mice examined (fig. S11A). Only 9 of the 36 regressing AV shunts exhibited loss of ECs. Twenty-seven AV shunts regressed without detectable loss of ECs (fig. S11B). We did detect EC loss later (fig. S11B), after AV shunt regression, but this was not correlated with either shunt diameter or degree of regression (fig. S11, C and D). An example of this is shown in Fig. 3B, where AV shunt regression was detected between 12 and 20 hours, but cell count was not reduced until 36 hours after Notch4* repression. These data suggest that the initiation of AV shunt regression does not require the loss of ECs.

Ex vivo staining for VE-cadherin, a marker of cell-cell junctions between ECs, in mutant mice before and after repression of *Notch4** suggests that the area encompassed by individual ECs was reduced during vessel regression (fig. S12). Therefore, mean area, but not the total number, of ECs was reduced during the acute regression of AV shunts after *Notch4** repression.

EphB4 is up-regulated in AV shunts after *Notch4** repression

We then asked whether recovery of venous specification, which was repressed in the presence of *Notch4**, might underlie the observed regression of AV shunts after *Notch4** repression. *Coup-TFII* is a venous marker that acts upstream of Notch. Therefore, we hypothesized that *Coup-TFII* expression would be retained in the cells of venous origin in the AV shunt, making it possible to trace the original venous segment and to assess the reestablishment of venous specification upon Notch4* repression. To determine *Coup-TFII* expression, we used a nuclear *lacZ* reporter of *Coup-TFII* promoter activity, *Coup-TFII*$^{+/fl\text{-}stop\text{-}nLacZ}$;*Tie2-Cre* (*5*). The *lacZ* expression is controlled by a floxed-STOP sequence. *Tie2-Cre*–mediated excision ensures that the *lacZ* reports the expression of *Coup-TFII* in *Tie2*$^{+}$ endothelial and hematopoietic cell lineages.

In wild-type control mice, *Coup-TFII* expression was localized to the EC nuclei of the venous branches, including capillaries, but was absent in the arterial branches in the brain (Fig. 4A). In mutant mice expressing *Notch4** (Fig. 4, B and C), regardless of whether *Notch4** was ON or OFF, *Coup-TFII* expression was maintained throughout the venous branches, as in control animals. Thus, *Coup-TFII* expression marked the venous boundary of AV shunts, suggesting that part of the AV shunts originated from the vein.

EphB4, in contrast to Coup-TFII, is a venous marker that acts downstream of Notch (*4*, *16*), making it possible to trace the effects of *Notch4** on the repression of venous specification. We used a *lacZ* reporter of *EphB4* promoter activity (*16*) to examine EphB4 expression before and after *Notch4** repression. In control mice, *EphB4*$^{tau\text{-}lacZ}$ was expressed throughout the veins, venules, and capillaries of the brain vasculature (Fig. 4D). *Notch4** expression decreased the expression of *EphB4*$^{tau\text{-}lacZ}$, resulting in patchy expression in the vein and very little expression in AV shunts (Fig. 4E).

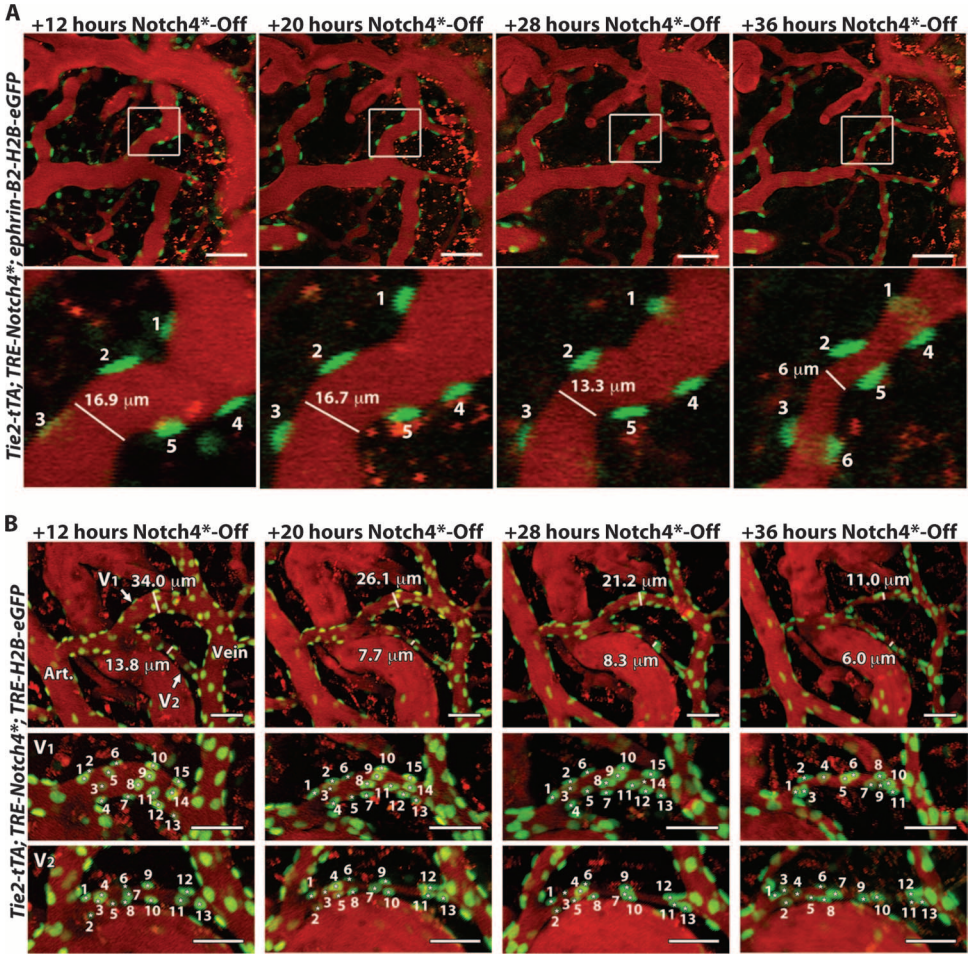

Fig. 3. Regression is initiated by reorganization of ECs. (**A**) Two-photon time-lapse imaging through a cranial window in mouse brain of nuclei marked by *ephrin-B2*$^{+/H2B\text{-}eGFP}$ in a *Notch4** mutant mouse. Plasma was labeled by intravenous Texas Red–dextran. In the AV shunt shown, vessel diameter was reduced by 28 hours after Notch4* repression, whereas the GFP$^+$ nuclei of ECs were retained after vessel regression at 36 hours. Because these images are Z-stacks through the vessel, cell 6 presented at 36 hours was also present earlier but out of the imaging plane. (**B**) Two-photon time-lapse imaging through a cranial window of nuclei marked by *Tie2-tTA/TRE-GFP* in a Notch4* mutant mouse. Plasma was labeled by intravenous Texas Red–dextran. In the AV shunt shown, vessel diameter was reduced by 20 hours after Notch4* repression, whereas the GFP$^+$ nuclei representing ECs were retained at 20 hours, and even at 28 hours when the vessel regressed further. At 36 hours, further regression was evident, and some EC loss was observed in the large shunt, V1, but not in the smaller shunt, V2. Scale bars, 50 μm.

To examine arterial marker expression during vessel regression, we used an ephrin-B2 reporter. We have previously shown that ephrin-B2 expression is up-regulated through the AV shunt in Notch4*-On mutants (*10*). Here, using *ephrin-B2*$^{tau\text{-}lacZ}$ reporter mice, we confirmed this up-regulation (Fig. 4H) and show that ephrin-B2 expression was normalized when Notch4* was turned off (Fig. 4I). To determine whether Notch4* repression leads to the normalization of a broader arterial specification program in the AV shunts, we examined the expression of additional arterial-specific proteins Dll4, Jag1, and Cx40 (Fig. 4, J to U). We found that all of these genes were expressed preferentially in the arteries in control mice; however, their expression extended throughout AV shunts and veins when Notch4* was switched on in mutant mice, and became normalized when Notch4* was switched off (Fig. 4, J to U).

These data, combined with the *Coup-TFII* expression pattern, suggest that *Notch4** induced arterial identity and repressed venous identity in the venous segment of AV shunts. Repression of *Notch4** resulted in the loss of the arterial markers ephrin-B2, Dll4, Jag1, and Cx40 (Fig. 4, I, O, R, and U, respectively) with a concomitant increase in *EphB4* expression in the regressing AV shunts (Fig. 4F).

To determine whether *EphB4* was re-expressed at the cellular level, we used the *TRE-H2B-eGFP* reporter to mark ECs in *Tie2-tTA;TRE-Notch4*;TRE-H2B-eGFP* mice expressing *Notch4** transgenes by eGFP expression (Fig. 5A). We found that EphB4 protein expression was repressed to ~50% of control levels in the *TRE-H2B-eGFP*$^+$ venous ECs of *Tie2-tTA;TRE-Notch4*;TRE-H2B-eGFP* mutant mice relative to *Tie2-tTA;TRE-H2B-eGFP* control mice. Once the Notch4* transgene was turned off, EphB4 expression normalized to control levels in the venous cell population.

Inhibition of EphB4 signaling impairs regression of AV shunts

To determine whether EphB4 signaling is necessary for the regression of AV shunts, we used a soluble form of the EphB4 (sEphB4) receptor to competitively inhibit EphB4 receptor signaling (*17*) after repression of *Notch4** (Fig. 5B). If regression depends on EphB4 signaling, sEphB4 receptor should inhibit the reduction in AV shunt diameter induced by suppression of *Notch4**. Indeed, the mean change in the diameter of AV shunts (−11.5% ± SD 20.8) was significantly reduced relative to mice not treated with sEphB4 (−49.3% ± SD 19.3, $P < 0.004$). As a control for the recombinant protein treatment, we examined AV shunt regression in mice injected with recombinant human fibronectin. The mean change in AV shunt diameter in these mice (39.7% ± SD 16.9) was not significantly different from the regression in mice without recombinant protein treatment ($P > 0.5$). Thus, sEphB4 significantly impaired the regression of AV shunts.

Regression of AV shunts alleviates hypoxia

To investigate the functional effect of AV shunt regression, we asked whether AV shunt regression reversed vascular dysfunction. We first examined blood velocity in arterial branches adjacent to the AV shunt and found that blood velocity increased with *Notch4** repression but decreased with continued *Notch4** expression (Fig. 2D). Markedly, these decreasing velocities could be promptly increased by *Notch4** repression and shunt regression (fig. S5). Perfusion of capillary vessels

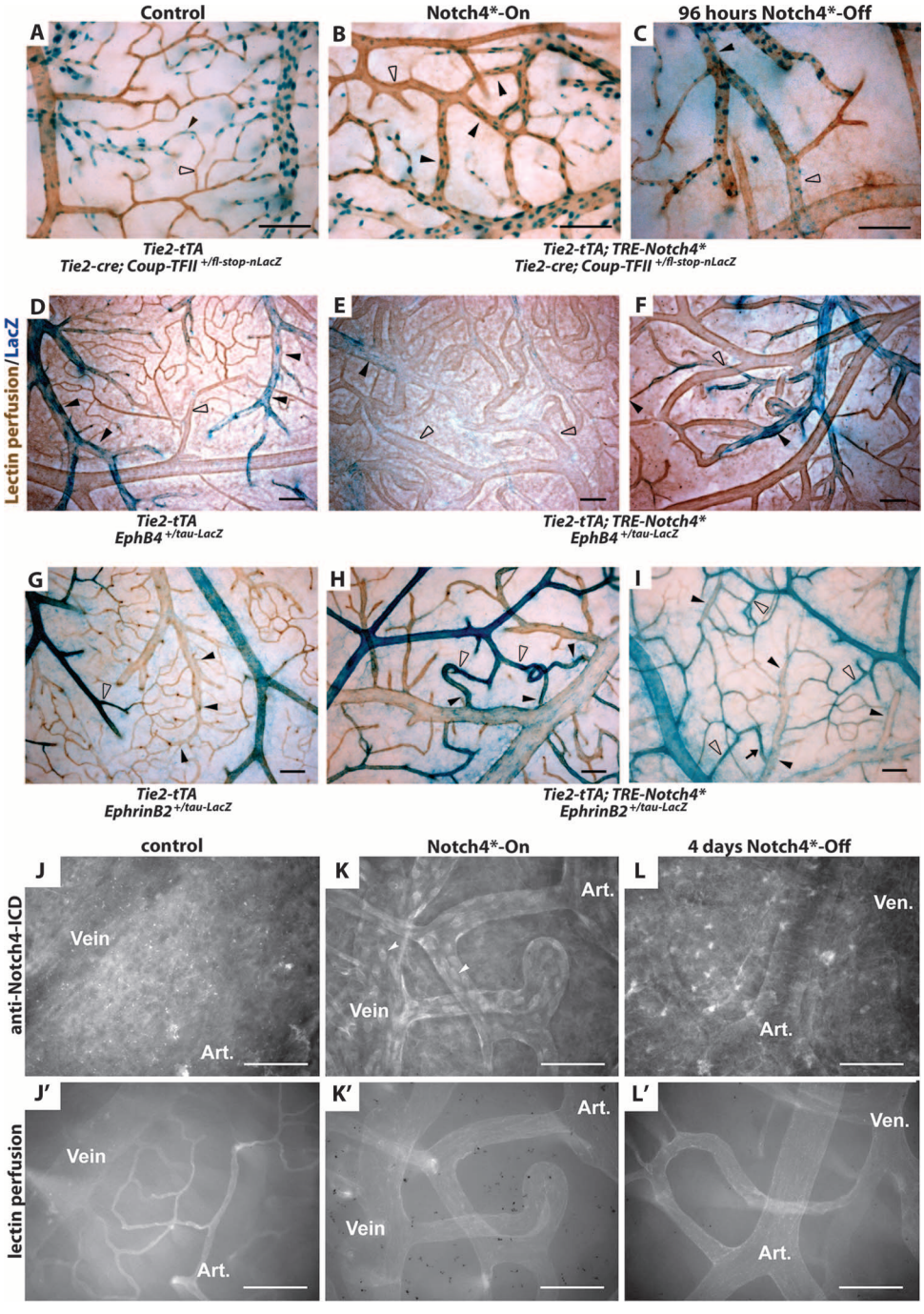

Fig. 4. Turning off Notch4* normalizes AV specification in AV shunts. (**A** to **I**) Whole-mount LacZ staining of the surface vasculature of the cerebral cortex reveals expression of Notch upstream venous specification gene *Coup-TFII*, downstream venous marker *EphB4*, and downstream arterial marker *ephrin-B2*. Perfused vessels were counterstained by colorimetric 3,3′-diaminobenzidine reaction with horseradish peroxidase–bound tomato lectin. (A to C) LacZ staining of *Tie2-cre* activated *Coup-TFII* reporter. (A) In control mice, *Coup-TFII* was expressed in the veins, venules, and capillaries up to the arterioles. (B) In *Notch4**-expressing mutants, *Coup-TFII* was expressed in the vein and venous portion of the AV shunt. (C) After repression of *Notch4**, the narrowest point in AV shunts was found between *Coup-TFII*–positive and *Coup-TFII*–negative endothelium. (D to F) LacZ staining of *EphB4* reporter. (D) In control mice, *EphB4* was expressed in the veins and venules up to the capillaries. (E) In *Notch4**-expressing mutants, *EphB4* expression was reduced through AV shunts, venules, and veins. (F) After the repression of *Notch4**, *EphB4* expression was increased in the regressing AV shunt. (G) In control mice, *ephrin-B2* expression was detected in the arteries and arterioles up to the capillaries. (H) In *Notch4**-expressing mutants, *ephrin-B2* expression was detected in the arteries, the AV shunts, and extending into the veins. (I) After repression of *Notch4**, *ephrin-B2* expression was decreased in the regressing AV shunts and veins. Closed arrowheads indicate venules; open arrowheads indicate arterioles. $n = 3$ (A to C, G, and I), $n = 4$ (H), and $n = 8$ (D to F) for each condition. Scale bars, 100 μm. (**J** to **U**) Whole-mount immunofluorescence staining of cerebral cortex after FITC-lectin perfusion. (J to L) Endothelial localization of Notch4-ICD was undetectable in control mice (J) but was present in a focal manner consistent with nuclear localization throughout the artery and vein in Notch4*-On mice (arrowheads in K); this was reduced once Notch4* was turned off (L). Arterial markers Dll4 (M to O), Jag1 (P to R), and Cx40 (S to U) were expressed in the artery but not the vein in control mice (M, P, and S). All of these markers were up-regulated in the artery, through the AV shunt, and into the vein in Notch4*-On mice (N, Q, and T). When Notch4* was turned off, the expression in the AV shunt and vein was lost but remained in the artery (O, R, and U). $n = 5$ for all mutants, $n = 2$ for each control. Scale bars, 100 μm. See next page for continuation of figure.

(Fig. 6, A to C) with a tomato lectin that binds to the endothelium suggests that tissue perfusion was globally increased after AV shunt regression.

Using hypoxyprobe staining, we then examined hypoxia in *Notch4** mutant mice with neurological defects before and after *Notch4** repression. The hypoxyprobe detects tissue exposed to a partial oxygen pressure of <10 mmHg, close to the hypoxic threshold expected to cause dysfunction of neuronal cells (*18*). We detected an increase in hypoxyprobe staining in the cerebellum and cerebral cortex of sick *Notch4**-expressing mice relative to their littermate controls (Fig. 6, D and F). When *Notch4** was repressed for 72 hours in severely affected *Notch4** mutant mice, hypoxyprobe staining intensity was significantly reduced, and approached that of control animals (Fig. 6E).

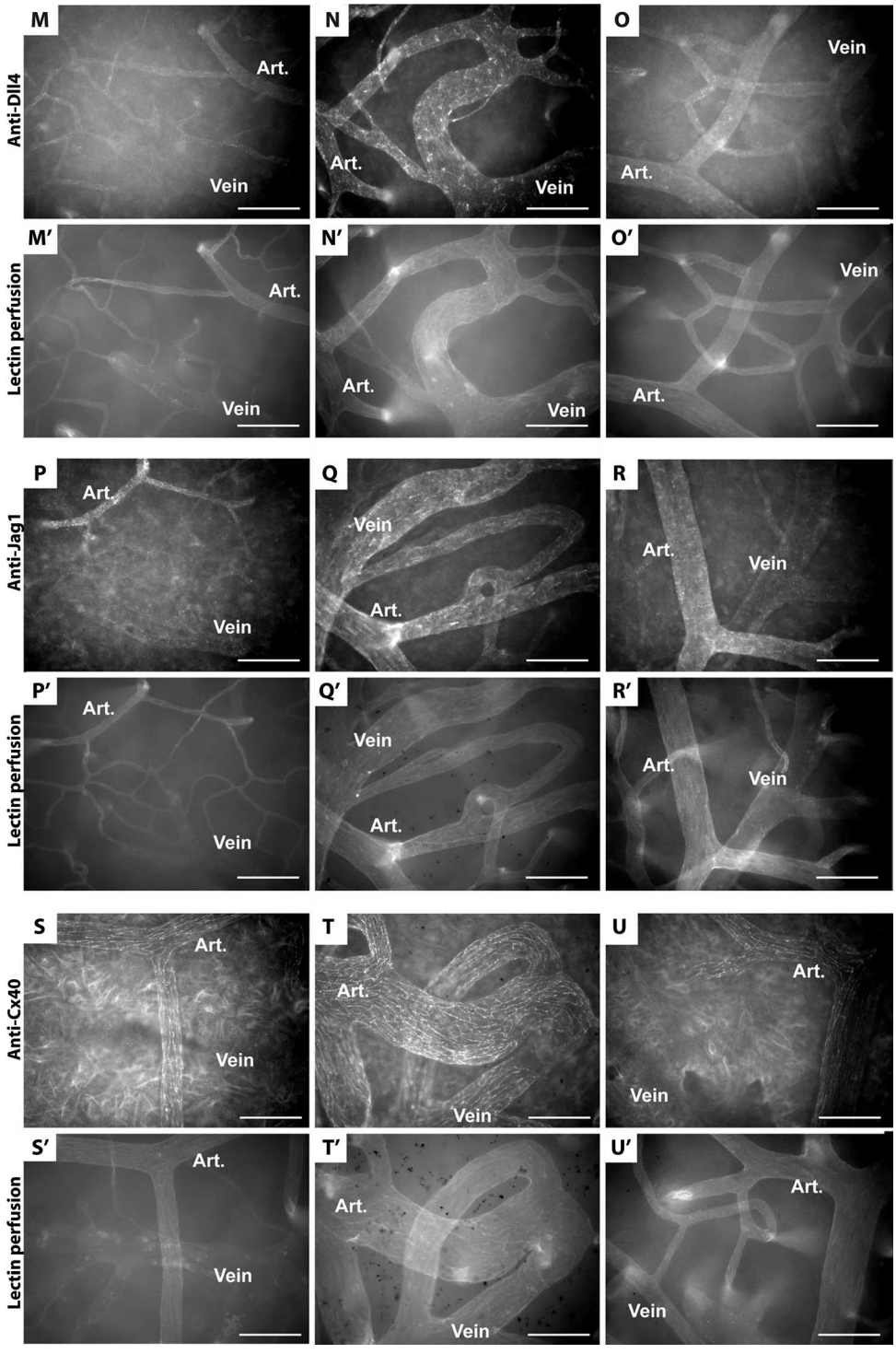

Fig. 4. Turning off Notch4* normalizes AV specification in AV shunts. (Continued from previous page)

Finally, we determined the histopathological changes in the brain parenchyma with and without *Notch4** repression. Histological analysis of *Notch4** mutant mice without *Notch4** repression revealed foci of pyknotic nuclei, often surrounding a core of decreased nuclear density, consistent with ischemia-induced necrosis (four of six mice, Fig. 6G). Such regions occasionally also contained evidence of hemorrhage. *Notch4** repression for several weeks eliminated these pyknotic and acellular regions (nine of nine mice), although structural damage could still be detected (Fig. 6H), presumably representing the evolution of the earlier ischemic damage. In support of this, hemosiderin deposits suggested the resolution of earlier hemorrhages. These findings suggest structural healing of earlier lesions after *Notch4** repression. Thus, regression of AV shunts induced by *Notch4** repression normalizes cerebrovascular flow patterns and tissue oxygenation, providing a physiological explanation for recovered brain function.

DISCUSSION

Here, we report that genetic reprogramming of AV specification converts high-flow AV shunts to low-flow microvessels. Using in vivo time-lapse imaging at single-cell resolution, we show that *Notch4** repression leads to a narrowing of AV shunts that was not dependent on loss of ECs, initiating AVM regression. Mechanistically, this involves the restoration of venous programming in the high-flow AV shunts by *Notch4** repression.

Notch induces reversible arterial programming of the venous compartment

Previously, we have observed expanded expression of the arterial marker *ephrin-B2* in the vasculature after up-regulation of Notch signaling in mice (*10*, *12*, *19*). Arterial ECs in coronary artery development have been reported to arise from venous vessels (*20*). However, it is currently unknown whether venous ECs had been reprogrammed to an arterial specification or whether arterial ECs had expanded. Using venous markers upstream (*Coup-TFII*) (*5*) and downstream (*EphB4*) (*19*) of Notch, we now show that Notch is sufficient to reprogram differentiated venous endothelium in the postnatal mouse. We show here, in normal brain endothelium, that *Coup-TFII* is preferentially expressed in venous but not arterial endothelium. Upstream of Notch, *Coup-TFII* expression is not affected by *Notch4** expression, identifying ECs of venous origin. Expression of *Notch4** led to the misexpression of the arterial markers ephrin-B2, Dll4, Jag1, and Cx40

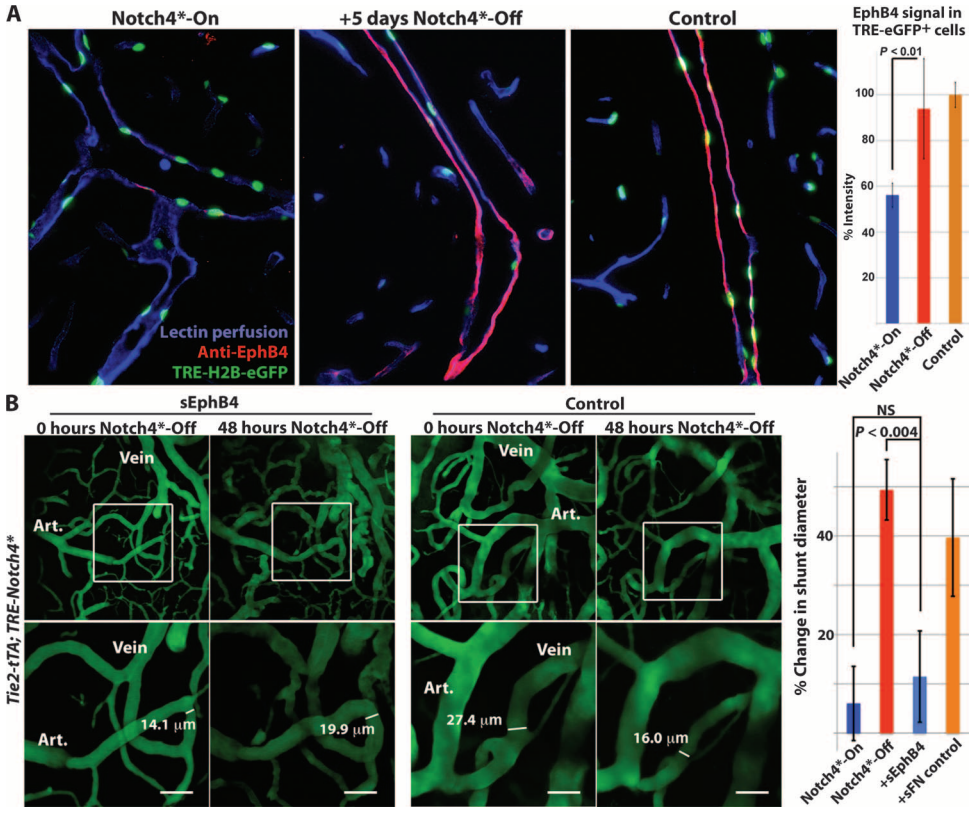

Fig. 5. Venous marker EphB4 is reexpressed in venous ECs and is required for AV shunt regression. (**A**) Sagittal sections showing veins in the cerebellum of *Tie2-tTA;TRE-Notch4*;TRE-H2B-eGFP* mutants before and 5 days after Notch4* repression, with littermate *Tie2-tTA;TRE-H2B-eGFP* control mice. EphB4 expression in TRE-eGFP$^+$ cells was visualized by immunofluorescence staining. EphB4 expression was selectively reduced in Notch4*-expressing mutant mice but recovered after Notch4* repression. Graph shows quantification of EphB4 fluorescence signal intensity in TRE-GFP$^+$ cells. n = 4 for mutants, n = 3 for controls, an average of ~12 cells per vessel and >5 vessels per mouse. (**B**) Two-photon time-lapse imaging of cortical brain vessels through a cranial window in *Notch4** mutant mice. Plasma was labeled by intravenous FITC-dextran. Treating *Notch4** mutant mice with soluble EphB4 (sEphB4) inhibited the regression of the AV shunt examined 48 hours after *Notch4** repression. In a *Notch4** mutant mouse littermate treated with soluble human fibronectin (sFN) as control, the AV shunt was reduced in diameter 48 hours after *Notch4** repression. Shown is quantification of changes in minimal AV shunt diameter after 48 hours in mice without repression of *Notch4** (*Notch4**-On, n = 35 AV shunts in 11 mice), with repression of *Notch4** (*Notch4**-Off, n = 22 AV shunts in 10 mice), with repression of *Notch4** and sEphB4 intravenous treatment (+sEphB4, n = 26 AV shunts in 5 mice), and with repression of *Notch4** and sFN control intravenous treatment (+sFN control, n = 13 AV shunts in 2 mice). Scale bars, 50 μm. Error bars represent SEM between individual AV shunts.

in Coup-TFII–positive veins, confirming that *Notch4** expression converts venous ECs into arterial ECs. Expression of *Notch4** also led to the suppression of the venous marker *EphB4* in the Coup-TFII–positive cells, demonstrating a simultaneous loss of venous expression in ECs of the venous lineage. Besides AV marker expression, venous segments converted by *Notch4** repression also exhibit the features of arteries, including arterial structure and flow velocity. Thus, our data suggest that Notch is sufficient to induce veins to become arteries.

We further demonstrate that this conversion of veins to arteries by Notch up-regulation is reversible. *Notch4** repression led to reexpression of the venous marker *EphB4* in *Coup-TFII*–positive vessels, as well as structural and hemodynamic normalization. Thus, our results suggest that venous vessels induced to become arteries by *Notch4** expression reverted back to veins after repression of *Notch4**. The reversible arterial specification in postnatal vasculature suggests that AV lineage specification is genetically pliable, and a single genetic manipulation is sufficient to switch AV specification postnatally.

AV reprogramming elicits narrowing of high-flow AV shunts without EC loss

The mechanism underlying the regression of AV shunts after *Notch4** repression involves *ephrin-B2* and *EphB4*-mediated EC reorganization, rather than a reduction of EC number. Although the role of *Eph/ephrin* signaling in the endothelium is not yet clear, our finding is consistent with the established functions of *ephrin-B2/EphB4* in regulating cell migration through repulsive signaling (*21*). We think that once reexpressed in *Coup-TFII*$^+$ ECs, *EphB4* mediates *ephrin-B2* signaling and elicits EC repulsion involving actomyosin contraction (Fig. 7). Supporting a critical role for *ephrin-B2/EphB4* signaling in this normalization process, the specific regression of vessels occurs at the AV interface, whereas the adjacent arteries often do not regress. Furthermore, the regression of AV shunts after *Notch4** repression can be blocked by sEphB4.

The mechanism of AV normalization after *Notch4** repression is distinct from the apoptotic mechanism of vessel regression after withdrawal of the growth factor VEGF (vascular endothelial growth factor). Microvessels in tumors and normal tissues regress after VEGF inhibition (*22*). Regression in these vessels is attributed to apoptosis of ECs (*23*). Another model of vessel regression is the hyaloid vasculature of the eye (*24*). In vivo imaging of hyaloid vessel regression shows that apoptosis of ECs obstructs the lumen and capillary blood flow, triggering the apoptosis of remaining ECs in the capillary segment and ultimately its regression (*25*). Thus, apoptosis and a subsequent reduction in blood flow are thought to precipitate vessel regression in these settings.

Our findings suggest that the cellular mechanism underlying the regression of the high-flow vessels after *Notch4** repression does not involve EC apoptosis, but likely is due to reorganization of ECs resulting from restoration of venous identity.

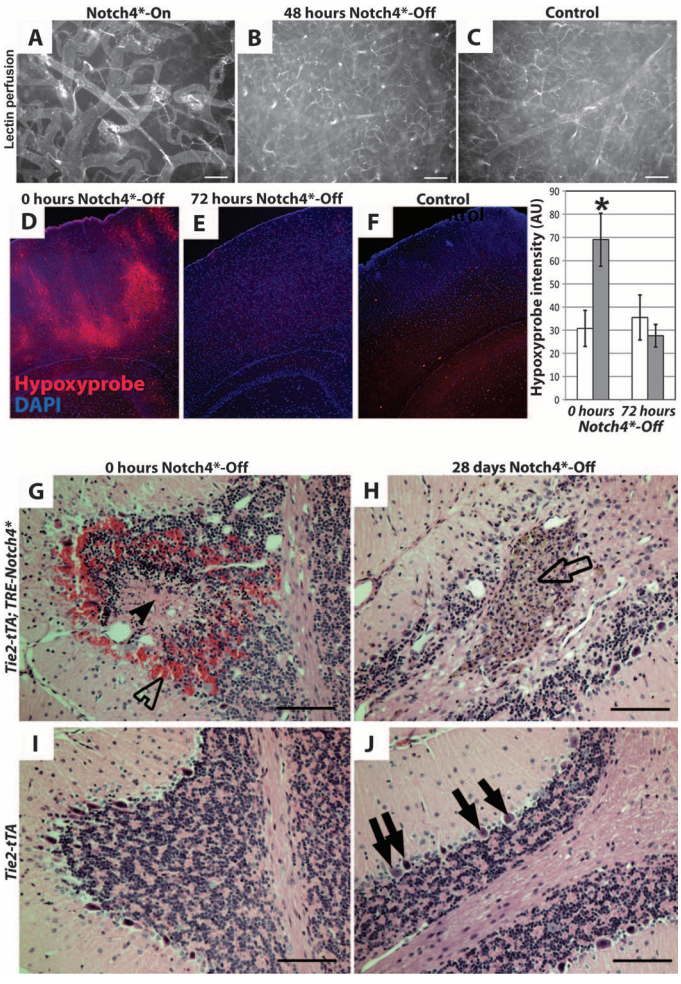

Fig. 6. *Notch4** repression normalizes vascular perfusion and tissue oxygenation. (**A** to **C**) Vascular perfusion of surface vessels of the cerebral cortex by fluorescent tomato lectin. After repression of *Notch4**, capillary perfusion was increased. (**D** to **F**) Immunofluorescence (red) staining for hypoxyprobe (pimonidazole) adduct in coronal section of mouse cortex. Patches of staining were visible in mutant mice with neurological defects before *Notch4** suppression (D). Staining was reduced 72 hours after suppression of *Notch4** (E). Control tissue shows an absence of staining (F). Quantification of staining intensity in cortical brain relative to nonspecific immunoglobulin G controls. Control before treatment is 30.8 arbitrary units (AU) ± SD 20.6; Notch4* mutant before treatment is 69.0 AU ± SD 34.2; control after treatment is 35.5 AU ± SD 25.6; Notch4* mutant after treatment is 27.6 AU ± SD 13.8. $P < 0.05$ versus all other groups by one-way analysis of variance (ANOVA) and Newman-Keuls multiple comparison test. $n = 9$ at 0 hours *Notch4**-Off, $n = 8$ at 72 hours *Notch4**-Off. (**G** to **J**) Hematoxylin and eosin staining of sagittal paraffin sections of cerebellum. In *Notch4** mutant mice before *Notch4** repression (0 hours *Notch4**-Off), areas of hemorrhage (open arrowhead) and necrotic tissue (closed arrowhead) were visible (G). After 28 days of *Notch4** suppression (28 days *Notch4**-Off), areas of scarring were visible (open arrow), but areas of hemorrhage and necrotic tissue had been resolved (H). The numbers of Purkinje cells were decreased in (H) when compared to these cells in the corresponding area in control (J) (solid arrows). Granular cells [open arrow in (H)] were found in the scarred area. Scale bars, 100 μm.

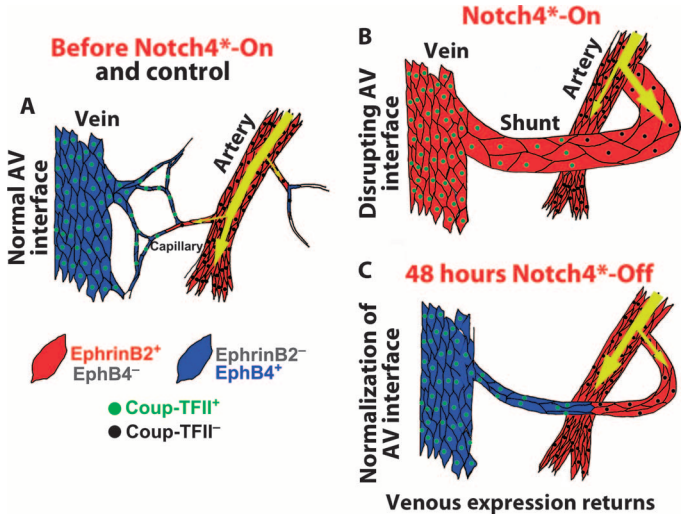

Fig. 7. Model for AVM regression after *Notch4** repression. (**A**) In control mice, Notch and ephrin-B2 are expressed in arteries and capillaries. Coup-TFII and EphB4 are expressed in veins and capillaries. (**B**) In mutant mice, *Notch4** is forcibly expressed throughout the endothelium, causing the repression of EphB4 and the expression of ephrin-B2 in AV shunts. The venous marker Coup-TFII, upstream of Notch, is retained, demarcating the original arterial-venous boundary. (**C**) Repression of *Notch4** allows EphB4 to be reexpressed in the Coup-TFII^{+} venous segment. Normalization of ephrin-B2/EphB4 signaling in ECs results in their reorganization, which initiates AV shunt narrowing and AVM regression.

Future implications

Direct in vivo imaging in this study demonstrates the regression of high-flow large vessels to capillary-like vessels by a single genetic manipulation that represses expression of *Notch4**. Markedly, vascular normalization was not accompanied by hemorrhage and vascular damage. Rather, AV shunt regression safely reversed tissue hypoxia and tissue dysfunction. We have focused on AVMs in mouse brain, but the finding likely applies to AVMs in other tissues given that we have previously identified *Notch4**-mediated AVMs in the liver, skin, uterus, and lung in the mouse (*12*, *19*, *26*). Thus, we believe that exploiting the tractable brain AVM mouse model system will provide important clues into the cellular and molecular regulation of AVMs in general. AV shunts are a core component of a range of high-flow vascular lesions (*1*). Thus, our demonstration of complete and safe normalization of dangerous high-flow AV shunts in animals may spur development of molecular therapeutic strategies to induce the regression of these dangerous high-flow vessels and treat these devastating diseases.

MATERIALS AND METHODS

Mice

Tie2-cre, *Tie2-tTA*, and *TRE-Notch4** mice are published (*8*, *10*, *12*, *19*), as are *ephrin-B2*$^{+/H2B\text{-}eGFP}$ (*27*), *EphB4*$^{+/tau\text{-}lacZ}$ (*16*), *ephrin-B2*$^{+/tau\text{-}lacZ}$ (*4*), *mT/mG* (*28*), *TRE-H2B-eGFP* (*29*), and *Coup-TFII*$^{+/fl\text{-}stop\text{-}nLacZ}$ mice (*30*). Tetracycline solution [Tet (0.5 mg/ml), sucrose (50 mg/ml), Sigma] was administered to mothers and withdrawn at birth (*10*). Doxycycline treatment was initiated with intraperitoneal injection

[500 μl of 1 mg/ml in phosphate-buffered saline (PBS)], followed by doxycycline diet (200 mg/kg, Bio-Serv) (*10*, *12*). All animals were treated in accordance with the guidelines of the University of California San Francisco Institutional Animal Care and Use Committee.

sEphB4 treatment

Two hundred microliters of recombinant human EphB4 extracellular domain (200 μg/ml) (R&D Systems) was injected by tail vein (final concentration of ~4 mg/kg), followed by 100 μl of 200 μg/ml 24 hours later (*17*). Recombinant human fibronectin (R&D Systems) at the same concentration was a negative control.

In vivo imaging

Chronic in vivo brain vascular imaging was performed as described (*11*, *31*), with modifications for immature mice (*32*). Briefly, a craniotomy was performed over the right cortex. A 5-mm glass coverslip (World Precision Instruments) was placed over artificial cerebrospinal fluid and fixed into place. A custom metal bar was attached adjacent to the window, allowing it to be secured by a custom adaptor arm on a stereotactic base (Cunningham). For imaging, mice were anesthetized with isoflurane (1.25 to 1.5%) in pure oxygen on a homeothermic heat blanket (Harvard Apparatus). Fluorescent contrast agents were injected by tail vein [2000-kD fluorescein isothiocyanate (FITC)–dextran (Sigma), 155-kD tetramethyl rhodamine isothiocyanate (TRITC)–dextran (Sigma), or 2000-kD Texas Red–dextran, prepared according to published protocols (*33*) and filtered by dialysis]. Two-photon microscopy was performed with a locally constructed microscope, to be described in detail in a future publication.

Immunostaining

Conjugated *Lycopersicon esculentum*–lectin (Vector Labs) was injected as we described (*10*, *12*). Brain was fixed by 1% paraformaldehye (PFA) fixation via the left ventricle. Tissue was incubated in blocking solution [2% bovine serum albumin (BSA), 0.1% Triton X-100 in PBS], primary antibody overnight, and secondary antibody overnight. Antibodies were anti–VE-cadherin (BD Pharmingen, clone 11D4.1, 1:200 dilution) and anti–α-smooth muscle actin (Sigma, clone 1A4, 1:200 dilution) (*12*, *34*). Staining for AV marker expression followed a similar protocol, except that blocking was with 10% donkey serum and 0.1% Triton X-100 in PBS. Antibodies (2 μg/ml in block) were anti–Notch4-ICD (intracellular domain) (Millipore), anti-Jag1 (R&D Systems), anti-Dll4 (R&D Systems), and anti-Cx40 (Santa Cruz).

Notch4 staining followed published protocols (*10*). Briefly, brains were perfusion-fixed with or without previous *L. esculentum*–lectin (Vector Labs) injection. After overnight fixation in 1% PFA, brains were sagitally bisected and dehydrated in 30% sucrose in PBS overnight and embedded in OCT (optimal cutting temperature). Sections (10 μm) were cut, blocked (3% donkey serum, 2% BSA, 0.2% Triton X-100 in PBS), and then incubated with anti–Notch4-ICD antibody (Millipore, formerly Upstate, 1:500 dilution) overnight in block, washed, incubated with secondary antibody, washed, and stored in VectaShield + DAPI (Vector Labs).

X-galactosidase/3,3′-diaminobenzidine co-staining

Under ketamine/xylazine and isoflurane anesthesia, 25 μg of biotinylated *L. esculentum*–lectin (Vector Labs) was injected via the inferior vena cava and allowed to circulate for 2 min. Perfusion was performed through the left ventricle with PBS, followed by fixative (0.25% glutaraldehyde, 50 mM EGTA, and 100 mM $MgCl_2$ in PBS). After short fixation, the cortex was stained for β-galactosidase at room temperature according to published X-galactosidase protocols (*35*). The cortex was then fixed with 1% PFA and blocked (10% BSA and 0.1% Triton X-100 in PBS), incubated with 1:1000 streptavidin-conjugated horseradish peroxidase (Jackson ImmunoResearch) in block, washed, and stained with a DAB (3,3′-diaminobenzidine) kit (Vector Labs).

SUPPLEMENTARY MATERIAL

www.sciencetranslationalmedicine.org/cgi/content/full/4/117/117ra8/DC1

Fig. S1. *Notch4** repression occurs within 24 hours of doxycycline treatment.
Fig. S2. Placement of the chronic imaging window.
Fig. S3. Specific regression of AV shunts after repression of *Notch4**.
Fig. S4. Repression of Notch4* induces regression of well-established large AV malformation.
Fig. S5. AV shunts are stable until repression of *Notch4**.
Fig. S6. AV shunts regress to capillary diameter vessels in mice with and without cranial window.
Fig. S7. Smooth muscle coverage is normalized by suppression of Notch4*.
Fig. S8. Velocity changes coincide with narrowing of AV shunts and distal vein beginning by 12 to 24 hours after *Notch4** repression.
Fig. S9. Narrowing of ephrin-B2–GFP^+ AV shunt occurs specifically after *Notch4** repression.
Fig. S10. *Tie2-tTA;TRE-H2B-eGFP* marks brain endothelial cells.
Fig. S11. Loss of endothelial cells is not required for AV shunt regression.
Fig. S12. Endothelial cells are narrowed in regressing AV shunts.

REFERENCES AND NOTES

1. M. C. Garzon, J. T. Huang, O. Enjolras, I. J. Frieden, Vascular malformations: Part I. *J. Am. Acad. Dermatol.* **56**, 353–370 (2007).
2. R. M. Friedlander, Clinical practice. Arteriovenous malformations of the brain. *N. Engl. J. Med.* **356**, 2704–2712 (2007).
3. C. Roca, R. H. Adams, Regulation of vascular morphogenesis by Notch signaling. *Genes Dev.* **21**, 2511–2524 (2007).
4. H. U. Wang, Z. F. Chen, D. J. Anderson, Molecular distinction and angiogenic interaction between embryonic arteries and veins revealed by ephrin-B2 and its receptor Eph-B4. *Cell* **93**, 741–753 (1998).
5. L. R. You, F. J. Lin, C. T. Lee, F. J. DeMayo, M. J. Tsai, S. Y. Tsai, Suppression of Notch signalling by the COUP-TFII transcription factor regulates vein identity. *Nature* **435**, 98–104 (2005).
6. D. Shin, G. Garcia-Cardena, S. Hayashi, S. Gerety, T. Asahara, G. Stavrakis, J. Isner, J. Folkman, M. A. Gimbrone Jr., D. J. Anderson, Expression of ephrinB2 identifies a stable genetic difference between arterial and venous vascular smooth muscle as well as endothelial cells, and marks subsets of microvessels at sites of adult neovascularization. *Dev. Biol.* **230**, 139–150 (2001).
7. R. Benedito, A. Duarte, Expression of *Dll4* during mouse embryogenesis suggests multiple developmental roles. *Gene Expr. Patterns* **5**, 750–755 (2005).
8. P. A. Murphy, G. Lu, S. Shiah, A. W. Bollen, R. A. Wang, Endothelial Notch signaling is upregulated in human brain arteriovenous malformations and a mouse model of the disease. *Lab. Invest.* **89**, 971–982 (2009).
9. Q. ZhuGe, M. Zhong, W. Zheng, G. Y. Yang, X. Mao, L. Xie, G. Chen, Y. Chen, M. T. Lawton, W. L. Young, D. A. Greenberg, K. Jin, Notch-1 signalling is activated in brain arteriovenous malformations in humans. *Brain* **132**, 3231–3241 (2009).
10. P. A. Murphy, M. T. Lam, X. Wu, T. N. Kim, S. M. Vartanian, A. W. Bollen, T. R. Carlson, R. A. Wang, Endothelial Notch4 signaling induces hallmarks of brain arteriovenous malformations in mice. *Proc. Natl. Acad. Sci. U.S.A.* **105**, 10901–10906 (2008).
11. C. B. Schaffer, B. Friedman, N. Nishimura, L. F. Schroeder, P. S. Tsai, F. F. Ebner, P. D. Lyden, D. Kleinfeld, Two-photon imaging of cortical surface microvessels reveals a robust redistribution in blood flow after vascular occlusion. *PLoS Biol.* **4**, e22 (2006).
12. T. R. Carlson, Y. Yan, X. Wu, M. T. Lam, G. L. Tang, L. J. Beverly, L. M. Messina, A. J. Capobianco, Z. Werb, R. Wang, Endothelial expression of constitutively active *Notch4* elicits reversible arteriovenous malformations in adult mice. *Proc. Natl. Acad. Sci. U.S.A.* **102**, 9884–9889 (2005).
13. M. Unekawa, M. Tomita, Y. Tomita, H. Toriumi, K. Miyaki, N. Suzuki, RBC velocities in single capillaries of mouse and rat brains are the same, despite 10-fold difference in body size. *Brain Res.* **1320**, 69–73 (2010).
14. E. A. Jones, F. le Noble, A. Eichmann, What determines blood vessel structure? Genetic prespecification vs. hemodynamics. *Physiology* **21**, 388–395 (2006).
15. E. Fuchs, The tortoise and the hair: Slow-cycling cells in the stem cell race. *Cell* **137**, 811–819 (2009).

16. S. S. Gerety, H. U. Wang, Z. F. Chen, D. J. Anderson, Symmetrical mutant phenotypes of the receptor *EphB4* and its specific transmembrane ligand *ephrin-B2* in cardiovascular development. *Mol. Cell* **4**, 403–414 (1999).
17. N. Kertesz, V. Krasnoperov, R. Reddy, L. Leshanski, S. R. Kumar, S. Zozulya, P. S. Gill, The soluble extracellular domain of EphB4 (sEphB4) antagonizes EphB4-EphrinB2 interaction, modulates angiogenesis, and inhibits tumor growth. *Blood* **107**, 2330–2338 (2006).
18. E. L. Rolett, A. Azzawi, K. J. Liu, M. N. Yongbi, H. M. Swartz, J. F. Dunn, Critical oxygen tension in rat brain: A combined ^{31}P-NMR and EPR oximetry study. *Am. J. Physiol. Regul. Integr. Comp. Physiol.* **279**, R9–R16 (2000).
19. Y. H. Kim, H. Hu, S. Guevara-Gallardo, M. T. Lam, S. Y. Fong, R. A. Wang, Artery and vein size is balanced by Notch and ephrin B2/EphB4 during angiogenesis. *Development* **135**, 3755–3764 (2008).
20. K. Red-Horse, H. Ueno, I. L. Weissman, M. A. Krasnow, Coronary arteries form by developmental reprogramming of venous cells. *Nature* **464**, 549–553 (2010).
21. M. E. Pitulescu, R. H. Adams, Eph/ephrin molecules—A hub for signaling and endocytosis. *Genes Dev.* **24**, 2480–2492 (2010).
22. R. K. Jain, Normalization of tumor vasculature: An emerging concept in antiangiogenic therapy. *Science* **307**, 58–62 (2005).
23. F. Baffert, T. Le, B. Sennino, G. Thurston, C. J. Kuo, D. Hu-Lowe, D. M. McDonald, Cellular changes in normal blood capillaries undergoing regression after inhibition of VEGF signaling. *Am. J. Physiol. Heart Circ. Physiol.* **290**, H547–H559 (2006).
24. I. B. Lobov, S. Rao, T. J. Carroll, J. E. Vallance, M. Ito, J. K. Ondr, S. Kurup, D. A. Glass, M. S. Patel, W. Shu, E. E. Morrisey, A. P. McMahon, G. Karsenty, R. A. Lang, WNT7b mediates macrophage-induced programmed cell death in patterning of the vasculature. *Nature* **437**, 417–421 (2005).
25. A. Meeson, M. Palmer, M. Calfon, R. Lang, A relationship between apoptosis and flow during programmed capillary regression is revealed by vital analysis. *Development* **122**, 3929–3938 (1996).
26. D. Miniati, E. B. Jelin, J. Ng, J. Wu, T. R. Carlson, X. Wu, M. R. Looney, R. A. Wang, Constitutively active endothelial Notch4 causes lung arteriovenous shunts in mice. *Am. J. Physiol. Lung Cell. Mol. Physiol.* **298**, L169–L177 (2010).
27. A. Davy, J. O. Bush, P. Soriano, Inhibition of gap junction communication at ectopic Eph/ephrin boundaries underlies craniofrontonasal syndrome. *PLoS Biol.* **4**, e315 (2006).
28. M. D. Muzumdar, B. Tasic, K. Miyamichi, L. Li, L. Luo, A global double-fluorescent Cre reporter mouse. *Genesis* **45**, 593–605 (2007).
29. T. Tumbar, G. Guasch, V. Greco, C. Blanpain, W. E. Lowry, M. Rendl, E. Fuchs, Defining the epithelial stem cell niche in skin. *Science* **303**, 359–363 (2004).
30. N. Takamoto, L. R. You, K. Moses, C. Chiang, W. E. Zimmer, R. J. Schwartz, F. J. DeMayo, M. J. Tsai, S. Y. Tsai, *COUP-TFII* is essential for radial and anteroposterior patterning of the stomach. *Development* **132**, 2179–2189 (2005).
31. A. Holtmaat, T. Bonhoeffer, D. K. Chow, J. Chuckowree, V. De Paola, S. B. Hofer, M. Hübener, T. Keck, G. Knott, W. C. Lee, R. Mostany, T. D. Mrsic-Flogel, E. Nedivi, C. Portera-Cailliau, K. Svoboda, J. T. Trachtenberg, L. Wilbrecht, Long-term, high-resolution imaging in the mouse neocortex through a chronic cranial window. *Nat. Protoc.* **4**, 1128–1144 (2009).
32. C. Portera-Cailliau, R. M. Weimer, V. De Paola, P. Caroni, K. Svoboda, Diverse modes of axon elaboration in the developing neocortex. *PLoS Biol.* **3**, e272 (2005).
33. S. Hornig, C. Biskup, A. Gräfe, J. Wotschadlo, T. Liebert, G. J. Mohr, T. Heinze, Biocompatible fluorescent nanoparticles for pH-sensoring. *Soft Matter* **4**, 1169–1172 (2008).
34. R. Braren, H. Hu, Y. H. Kim, H. E. Beggs, L. F. Reichardt, R. Wang, Endothelial FAK is essential for vascular network stability, cell survival, and lamellipodial formation. *J. Cell Biol.***172**, 151–162 (2006).
35. B. Carpenter, Y. Lin, S. Stoll, R. L. Raffai, R. McCuskey, R. Wang, VEGF is crucial for the hepatic vascular development required for lipoprotein uptake. *Development* **132**, 3293–3303 (2005).

Acknowledgments: We thank C. Tomas-Miranda and W. Jiang for experimental assistance, S. Tsai for the *Coup-TFII*$^{+/fl\text{-}stop\text{-}nLacZ}$ mice, R. Daneman for critical reading, and members of our laboratory for helpful discussions. **Funding:** This work was supported by the Foundation for Accelerated Vascular Research (formerly the Pacific Vascular Research Foundation), the Frank A. Campini Foundation, the Mildred V Strouss Trust, NIH R01 HL075033, NIH RO1 NS067420, and American Heart Association (AHA) grant-in-aid 10GRNT4170146 to R.A.W.; AHA 0715062Y and Tobacco-Related Disease Research Program (TRDRP) 18DT-0009 Predoctoral Fellowships to P.A.M.; TRDRP 19DT-007 and NIH F30 1F30HL099005-01A1 Predoctoral Fellowships to T.N.K.; and the University of California San Francisco Liver Center Morphology Core supported by NIH P30-DK026743. **Author contributions:** P.A.M., R.A.W., and T.N.K. designed the experiments; P.A.M., T.N.K., and G.L. performed the experiments; P.A.M., R.A.W., T.N.K., G.L., and A.W.B. analyzed the data; T.N.K., C.B.S., and P.A.M. contributed tools and technology; and P.A.M. and R.A.W. wrote the paper. **Competing interests:** The authors declare that they have no competing interests.

Submitted 17 May 2011
Accepted 22 December 2011
Published 18 January 2012
10.1126/scitranslmed.3002670

Citation: P. A. Murphy, T. N. Kim, G. Lu, A. W. Bollen, C. B. Schaffer, R. A. Wang, *Notch4* normalization reduces blood vessel size in arteriovenous malformations. *Sci. Transl. Med.* **4**, 117ra8 (2012).